Letter

Transmission zeros with topological symmetry in complex systems

Yuhao Kang (康雨毫) and Azriel Z. Genack*

Queens College and The Graduate Center of the City University of New York, Flushing, New York 11367, USA

(Received 24 June 2020; revised 10 February 2021; accepted 12 February 2021; published 1 March 2021)

Understanding vanishing transmission in Fano resonances in quantum systems and metamaterials and perfect and ultralow transmission in disordered media has advanced the knowledge and applications of wave interactions. Here, we use analytic theory and numerical simulations to understand and control the transmission and transmission time in complex systems by deforming a medium and adjusting the level of gain or loss. Unlike the zeros of the scattering matrix, the position and motion of the zeros of the determinant of the transmission matrix (TM) in the complex plane of frequency and field decay rate have robust topological properties. In systems without loss or gain, the transmission zeros appear either singly on the real axis or as conjugate pairs in the complex plane. As the structure is modified, two single zeros and a complex conjugate pair of zeros may interconvert when they meet at a square root singularity in the rate of change of the distance between the transmission zeros in the complex plane with sample deformation. The transmission time is the spectral derivative of the argument of the determinant of the TM. It is a sum over Lorentzian functions associated with the resonances of the medium, which is the density of states, and with the zeros of the TM. Transmission vanishes, and the transmission time diverges as zeros are brought near the real axis. Monitoring the transmission and transmission time when two zeros are close may open new possibilities for ultrasensitive detection.

DOI: 10.1103/PhysRevB.103.L100201

I. INTRODUCTION

There has been longstanding interest in understanding the suppression of scattering in quantum and classical systems. The increasing power of nanofabrication and the continuing discovery of novel properties of waves in metamaterial has heightened interest in exploiting singularities in the scattering matrix (SM) [1–3] or in portions of the SM, such as the reflection matrix (RM) [4], for applications to sensing, switching, lasing, and energy deposition [1–4]. The singularities of the SM in unitary systems are complex conjugate pairs of poles and zeros in the complex energy or frequency plane. Incident radiation is completely absorbed when a zero of the SM is brought to the real axis. Such coherent perfect absorption (CPA) [1,5–10] is the time reversal of an outgoing wave at the lasing threshold. Lasing and CPA may occur simultaneously in a parity-time (PT)-symmetric system in which a pole and its conjugate zero are brought to the real axis together [11,12].

Zero reflection is also achieved in any subset of input channels when zeros of the RM are on the real axis [4,13]. The reflection zeros may be found anywhere in the complex plane. The reflection time difference (RTD) between the two sides of a quasi-one-dimensional (1D) sample can be expressed as a sum of Lorentzians associated with the reflection zeros [14,15]. This is a counterpoint to the Wigner time delay, which can be expressed as the sum of resonances corresponding to Lorentzian functions for the poles [16].

The transmission matrix (TM) was developed to explain the scaling of conductance in the quasi-1D wire geometry [17] but has been intensively studied recently because it allows the control of transmission of classical waves [18–23]. The question naturally arises as to whether zeros exist in the TM as they do in the SM and the RM. For the SM and the RM, the determinant of the matrix involves a numerator which is a single determinant, while the numerator of the determinant of the TM involves a product of determinants, so that the path to a transmission zero (T-zero) is not apparent. However, we will see that it is from this added complexity that unique topological constraints emerge that make it easy to visualize and control the motion of T-zeros.

Fano resonances are a subset of the complex T-zero in which the T-zeros fall on the real axis in the complex plane. Fano's analysis [24] was introduced to explain inelastic electron scattering in helium but has been applied beyond atomic physics to nuclear and condensed matter physics, electronics, and optics [25,26]. The steep asymmetric drop to zero in spectra of Fano resonances arises from the interference of a narrow mode and a continuum or broad mode [24,25,27–29].

In multichannel media, it is possible to achieve perfect transmission in the highest transmission eigenchannel with eigenvalue of the matrix $tt^\dagger$ of unity $\tau_1 = 1$ by judiciously manipulating the incident wave, where t is the $N \times N$ TM [17,18,22]. Ultralow transmission in the lowest transmission eigenchannel [17,18,30–32] is due to interference of far-off-resonance modes [8]. The average of the lowest transmission eigenchannel τ_N is $e^{-2L/l}$, where L is the sample length and l is the transport mean free path [17,30,31,33]. Whether transmission can be identically zero has remained an open question. We will show that the transmission of the lowest transmission eigenchannel of a quasi-1D sample can vanish when the T-zeros are on the real axis.

*Corresponding author: genack@qc.edu

In this paper, we demonstrate the topological structure of zeros of the TM. While the TM has the same poles as the SM and RM, the symmetry properties of the T-zeros are entirely different. Like their conjugate partners, the poles, the zeros of the SM are not associated with any symmetry within the complex plane, while the zeros of the RM only exhibit a symmetry relative to the real axis in systems with PT symmetry [4]. In contrast, T-zeros have mirror symmetry relative to the real axis in lossless random systems. This unique property requires that, in a unitary medium, the T-zeros appear either as single zeros on the real axis or as complex conjugate pairs. The single zeros are topologically constrained to move on the real axis with deformation of the sample. They may only leave or arrive at the real axis when two single zeros meet and interconvert with a conjugate pair of zeros. The rate of change of the frequency of single zeros and of the distance from the real axis of the conjugate pair near this degenerate zero point (ZP) diverges. Changes in the sample near the ZP can in principle be detected with ultrahigh sensitivity. This is analogous to the heightened sensitivity that arises when two poles approach an exceptional point (EP) [34,35], but the approach to the ZP can be readily achieved and monitored. Because of the symmetry of T-zeros in unitary systems, the transmission time is proportional to the density of states (DOS), which is a sum of Lorentzian lines associated with the poles or resonances. In the presence of loss or gain, however, the zeros are manifest in the spectrum of transmission time as Lorentzian lines with linewidths which vanish as the zeros are brought to the real axis. The prospects for ultrasensitive detection of perturbations near a ZP are discussed.

A. Symmetry of transmission zeros

The TM t is a quadrant of the SM $S=\begin{bmatrix} r & t' \\ t & r' \end{bmatrix} = \begin{bmatrix} V & \\ & U \end{bmatrix}\begin{bmatrix} -\sqrt{1-\tau} & \sqrt{\tau} \\ \sqrt{\tau} & \sqrt{1-\tau} \end{bmatrix}\begin{bmatrix} V^\dagger & \\ & U^\dagger \end{bmatrix}$. Here, τ is the diagonal matrix of transmission eigenvalues, and U and V are unitary matrices [23]. In 1D, the transmission time is the spectral derivative of the phase of the transmitted field $\tau_{\mathrm{T}}=\frac{d\arg(t)}{dE}$, where $\hbar=1$, and E is the angular frequency ω for classical waves [36–40]. Generalizing this relation to quasi-1D gives $\tau_{\mathrm{T}}=\frac{d}{dE}\mathrm{argdet}(t)$. We show in Sec. I of the Supplemental Material [41] that, in a lossless medium, this relation gives $\tau_{\mathrm{T}}=\pi\rho$, where ρ is the DOS [42,43].

To separate the impacts of resonances and zeros upon the transmission time, we employ the Heidelberg model [16,44–48], in which the SM is expressed as $S=\frac{I-iK}{I+iK}$, where $K=\pi W^\dagger\frac{1}{E-H_{\mathrm{in}}}W$. Here, H_{in} is the internal Hamiltonian of the scattering region, and W is the coupling matrix between the channels in the leads and the modes within the medium. The coupling between the N channels in the leads and the M quasinormal modes of the system within the spectral range of interest is given via the matrix $W=[W_1 \quad W_2]$, where the $M\times N$ matrix $W_{1/2}$ couples the scattering region and the surroundings. The expression for the determinant of the TM is obtained in Sec. II of the Supplemental Material [41]

$$\det(t)=(-2\pi i)^N\frac{\det(E-H_{\mathrm{in}})\det\left(W_2^\dagger\frac{1}{E-H_{\mathrm{in}}}W_1\right)}{\det(E-H_{\mathrm{eff}})}, \tag{1}$$

where $H_{\mathrm{eff}}=H_{\mathrm{in}}-i\pi WW^\dagger$ is the effective Hamiltonian of the scattering region.

Similarly, for transmission from the right to left sides, $\det(t')=(-2\pi i)^N\det(E-H_{\mathrm{eff}})^{-1}\det(E-H_{\mathrm{in}})\det(W_1^\dagger\frac{1}{E-H_{\mathrm{in}}}W_2)$.

The numerator in Eq. (1), $Y=\det(E-H_{\mathrm{in}})\det(W_2^\dagger\frac{1}{E-H_{\mathrm{in}}}W_1)$ points to the condition of zero transmission. However, Y does not have a clear physical meaning and contains the inverse of $E-H_{\mathrm{in}}$. In contrast, the operator for zeros of the SM is $Y_S=\det(E-H_{\mathrm{in}}-i\pi WW^\dagger)$, and the operator for the zeros of the RM is $Y_R=\det(E-H_{\mathrm{in}}+i\pi W_2W_2^\dagger-i\pi W_1W_1^\dagger)$. Both operators have a straightforward physical meaning. When CPA is achieved, all channels provide effective gain, so that the effective internal Hamiltonian is $H_{\mathrm{in}}+i\pi WW^\dagger$. For the reflectionless case, the input channel acts as effective gain, and the output acts as effective loss; thus, the effective internal Hamiltonian is $H_{\mathrm{in}}-i\pi W_2W_2^\dagger+i\pi W_1W_1^\dagger$ [4].

In contrast, the numerator of the TM has the unique property that it is real for real E. In a reciprocal system, $t^T=t'$, so that $\det(W_2^\dagger\frac{1}{E-H_{\mathrm{in}}}W_1)=\det(W_1^\dagger\frac{1}{E-H_{\mathrm{in}}}W_2)$. When, in addition, the system does not possess internal loss or gain, $H_{\mathrm{in}}^\dagger=H_{\mathrm{in}}$. When E is on the real axis, $(W_2^\dagger\frac{1}{E-H_{\mathrm{in}}}W_1)^\dagger=W_1^\dagger\frac{1}{E-H_{\mathrm{in}}}W_2$. Combining these equations, we find for a unitary reciprocal system that $\det(W_2^\dagger\frac{1}{E-H_{\mathrm{in}}}W_1)$ is real for real E.

Furthermore, as shown in Sec. II of the Supplemental Material [41], the numerator of Eq. (1) can be expressed as $\prod_{i=1}^{M-N}(E-\eta_i)$. Here, the $\eta_i=Z_i+i\zeta_i$ denote the zeros of $\det(t)$, while the denominator is given by $\det(E-H_{\mathrm{eff}})=\prod_n(E-\lambda_n)$, where $\lambda_n=E_n-i\gamma_n$ are the poles of the resonances, and γ_n is the halfwidth of the mode. This yields the factorized expression

$$\det(t)\sim\frac{\prod_{i=1}^{M-N}(E-\eta_i)}{\prod_{j=1}^{M}(E-\lambda_j)}. \tag{2}$$

Since the transmission time is given by $\tau_{\mathrm{T}}=\frac{d}{dE}\mathrm{argdet}(t)$, the sum of the contributions from poles and zeros is

$$\tau_{\mathrm{T}}=\tau_p+\tau_z=\sum_n\frac{\gamma_n}{(E-E_n)^2+\gamma_n^2}+\sum_i\frac{\zeta_i}{(E-Z_i)^2+\zeta_i^2}. \tag{3}$$

Since $\prod_{i=1}^{M-N}(E-\eta_i)$ is always real for real E in a unitary system, the η_i must be disposed symmetrically with respect to the real axis. The zeros are therefore either real or part of a conjugate pair. Therefore τ_z vanishes in a unitary system and τ_{T} is due solely to the poles, which is the DOS [16,43].

The symmetry of the η_i is broken by loss or gain so that τ_z no longer vanishes. For a system with uniform internal loss or gain, $H_{\mathrm{in}}=H_0-i\gamma$, the position of the zeros of $\det(t)$ shifts down by $i\gamma$, giving $\eta_i'=\eta_i-i\gamma$. The contribution of a single zero to τ_{T} is $\tau_z=\frac{-\gamma}{(E-Z)^2+\gamma^2}$, with peak value $-\gamma^{-1}$. For a conjugate pair of zeros in a unitary medium, $\eta=Z\pm i\zeta$, the corresponding zeros for the nonunitary system are at $\eta'=Z+i(\pm\zeta-\gamma)$. A pair of zeros then contribute to the transmission time with $\tau_z=\frac{-\zeta-\gamma}{(E-Z)^2+(-\zeta-\gamma)^2}+\frac{\zeta-\gamma}{(E-Z)^2+(\zeta-\gamma)^2}$, giving a local extremum at $E=Z$ of $\frac{2\gamma}{\zeta^2-\gamma^2}$. When a T-zero is near the real axis of the complex energy plane, a narrow Lorentzian peak appears in the spectrum of the

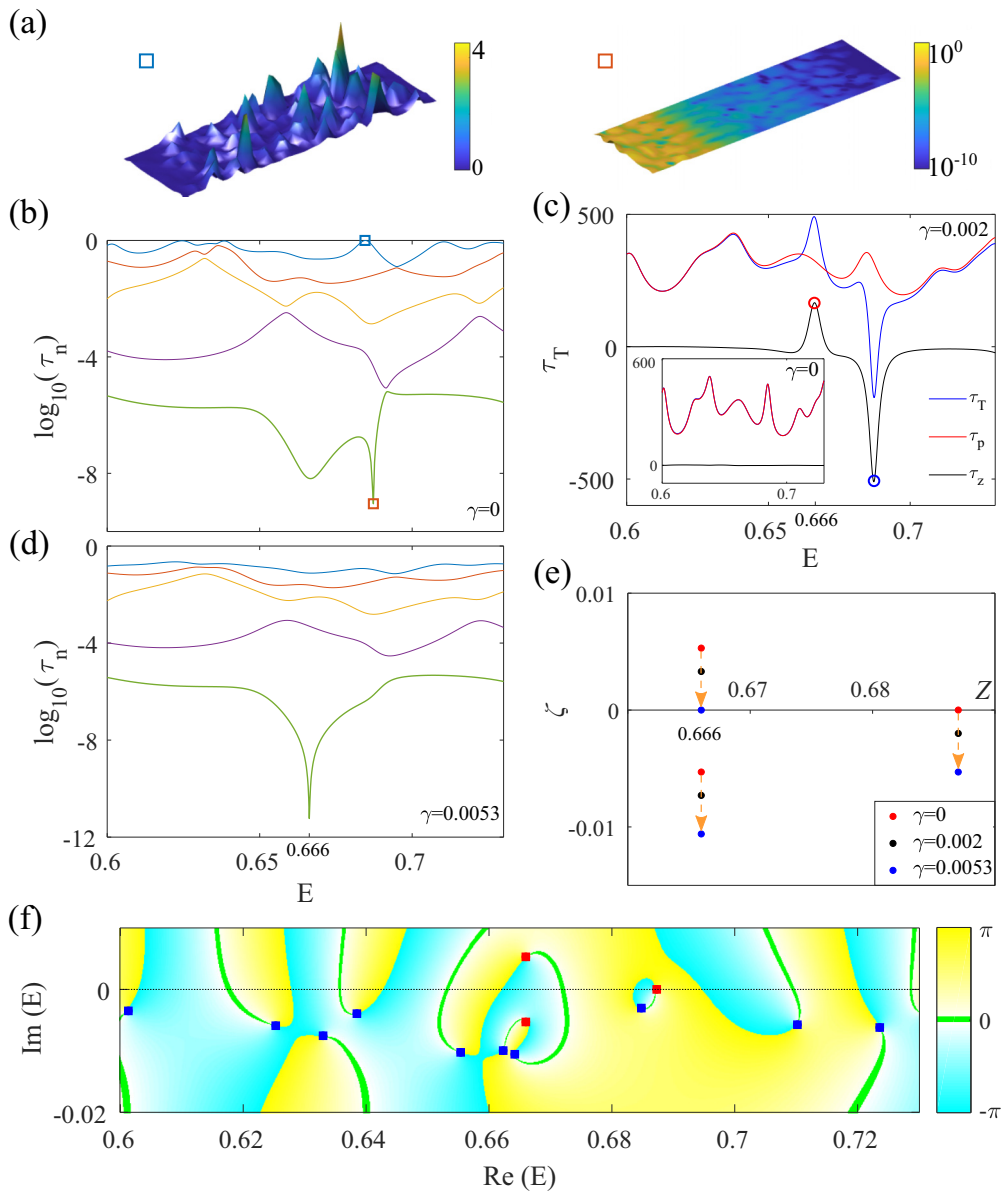

FIG. 1. Transmission zeros in a random quasi-one-dimensional (1D) sample. Simulations are carried out in a sample of width 20 and length 60 which supports five channels in the energy range of the simulation. (a) Intensity profile for the perfectly transmitting eigenchannel at $E = 0.6845$ and the eigenchannel with vanishing transmission at $E = 0.6873$ indicated, respectively, by the blue and red squares, in (b). The color bar is linear for the first pattern and logarithmic for the second pattern. (b) Spectra of the five transmission eigenvalues in the lossless system. (c) Transmission times for onsite loss $\gamma = 0.002$. τ_p is calculated by integrating the imaginary part of the local Green's function $\tau_p = -\int \mathrm{Im}G(r, r, E)d\vec{r}$, which is the local density of states (DOS). $\tau_z = \tau_T - \tau_p$ is given by the black curve. The inset shows that τ_p and τ_T coincide, with $\tau_z = 0$ in the lossless system. (d) Lossy system with $\gamma = 0.0053$ in which one transmission zero lies on the real axis at $E = 0.666$ with $\tau_N = 0$. (e) Displacement of three transmission zeros in the complex plane for the losses in (b)–(d). (f) Phase map of $\arg\det(t)$ in the complex energy plane. Red (blue) squares indicate transmission zeros (poles).

transmission time. Thus, counterintuitively, narrow spectral lines or even discontinuities are produced by adding absorption.

The divergence of transmission time when a T-zero is near the real axis can be understood by the complex representation of the trajectory of the transmitted field vs frequency in a double mode system (Fig. S1b of the Supplemental Material [41]). In Sec. III of the Supplemental Material [41], we discuss the divergence of the transmission time when the trajectory of the transmitted field is near the origin.

We note that Eq. (3) remains valid even when a nonresonant part of field contributes to the transmission, for instance, in the interference between a coherent wave and a resonant mode (Sec. IV of the Supplemental Material [41]). In general, τ_z does not vanish in a nonunitary system; however, it can vanish in a 1D PT-symmetric system [11,49] with balanced loss and gain (Sec. V of the Supplemental Material [41]).

B. Transmission zeros in a quasi-1D system

We first explore the impact of transmission zeros on the transmission and transmission time in a random quasi-1D sample. We carry out simulations for a quasi-1D system using the tight-binding model simulated with the open-source package Kwant [50] for a sample with $N = 5$. The results for a system in which the onsite energy is 4 in the uniform leads and distributed randomly within the scattering region over $[4 - w,\ 4 + w]$, with $w = 1.1$, and nearest neighbor coupling -1 are shown in Fig. 1. The profiles of energy density of the transmission eigenchannels with perfect and vanishing transmission in a lossless sample are shown in Fig. 1(a) for points in the spectra of the transmission eigenvalues indicated by the squares in Fig. 1(b).

The inset in Fig. 1(c) shows that τ_{T} and τ_p coincide in the lossless system, with $\tau_z = 0$. With uniform internal loss of $\gamma = 0.002$, however, τ_{T} and τ_p differ, as shown in the spectrum of $\tau_z = \tau_{\mathrm{T}} - \tau_p$ in Fig. 1(c). The imaginary coordinates of the transmission zeros can be determined from the extrema in τ_z. The peak of τ_z indicated by the red circle in Fig. 1(c) shows that one of the zeros of a pair is slightly above the real axis. The value at the peak of τ_z, $\frac{2\gamma}{\zeta^2-\gamma^2}$ gives $\zeta = 5.3 \times 10^{-3}$. Thus, the upper T-zero of the pair at $E = 0.666$ would be moved to the real axis by adding loss of $\gamma = 5.3 \times 10^{-3}$. At this energy, the lowest transmission eigenchannel vanishes $\tau_N = 0$, as indicated by the dip in τ_N in Fig. 1(d).

Simulation of transmission in the lossless system does not allow a definitive determination of whether the lowest transmission eigenchannel is identically zero. This can be determined, however, from the depth of the dip of τ_z when absorption is added. For a single real transmission zero in the lossless system, τ_z would dip to $\gamma^{-1} = 500$, as is indeed found in Fig. 1(c). If $\det(t)$ at this frequency in the lossless sample were merely exponentially small, there would be a pair of conjugated zeros close to the real axis, which would give a dip of $2\gamma^{-1} = 1000$. The dip of 500 allows us to conclude that the smallest transmission eigenvalue at the blue circle is identically zero in the lossless case.

There are three transmission zeros within the energy range of Fig. 1. Their positions are shown in Fig. 1(e) as the upper zero of the pair is moved to the real axis. Both transmission zeros and poles are topological phase singularities. The phase of $\det(t)$ can be seen in the phase map of Fig. 1(f) to increase (decrease) by 2π in a counterclockwise rotation about the transmission zeros (poles), which are indicated by red (blue) squares. The phase singularities correspond to topological charges of $+1$ for each zero. The topological charge of the T-zero is conserved, as it is for phase singularities in the speckle pattern of scattered waves [51–53].

C. Transmissionless mode and phase transition of transmission zeros

We now consider the motion of transmission zeros with displacement of an element of the sample. The sample is a lossy billiard with reflecting disks coupled to its surroundings via two single-channel leads. The lowest disk is displaced, as shown in Fig. 2(a). The positions of the poles are found using COMSOL mode solver and the harmonic inversion method [54,55]. Figure 2(b) shows the zeros of a pair approaching each other on a curved trajectory as the lowest disk is displaced to the right. The zeros remain equidistant from the line $\zeta = -i\gamma$ along the trajectory and meet on the line at a ZP. At the ZP, the phase changes by 4π in a counterclockwise circuit of the zeros, so that the topological charge is conserved as the paired zeros are transformed to single zeros, as can be seen in Fig. 2(c). With further displacement of the disk, two single zeros appear and move along the line $\zeta = -i\gamma$. It is noteworthy that the poles seen in Fig. 2(c) hardly move for the small displacement in which a pair of zeros is converted to two single zeros.

One of the T-zeros of a pair can be brought to the real axis in an absorbing medium by deforming the sample, as indicated by the star in Fig. 2(b). The profiles of intensity and

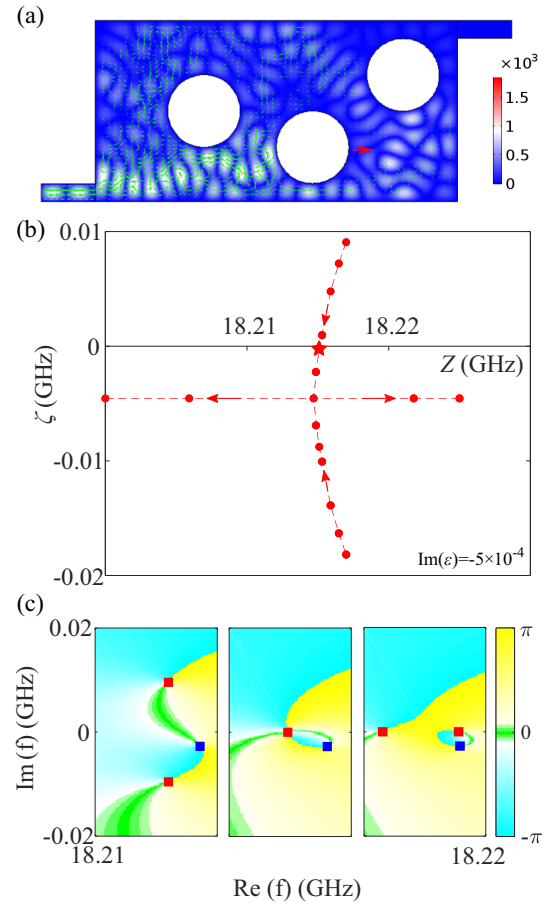

FIG. 2. Interconversion of single and paired transmission zeros in a lossy billiard. (a) Profiles of energy flow and field amplitude at the T-zero indicated by the star in (b). The length of the arrows indicates the logarithm of the flux. The amplitude of the field is given by the color bar on the right. The permittivity in the system is $\varepsilon = 1 - 5 \times 10^{-4} i$. The sample width and length are 10 and 20 cm. The leads have a width of 1 cm. The diameter of the disk is 4 cm. (b) Trajectories of two transmission zeros with x coordinates of the center of the lowest disk at 1.996, 1.998, 2, 2.002, 2.0024, 2.0028, 2.003, 2.005, and 2.008 (cm). The two zeros meet at zero point (ZP) when $x = 2.003$ cm. The star indicates the transmissionless mode in the lossy system. (c) Phase diagram of transmission between 18.21 and 18.22 GHz when the lowest disk is at 2.000 cm (left), at 2.003 cm (middle, ZP), and 2.0033 cm (right). Red (blue) squares indicate transmission zeros (poles).

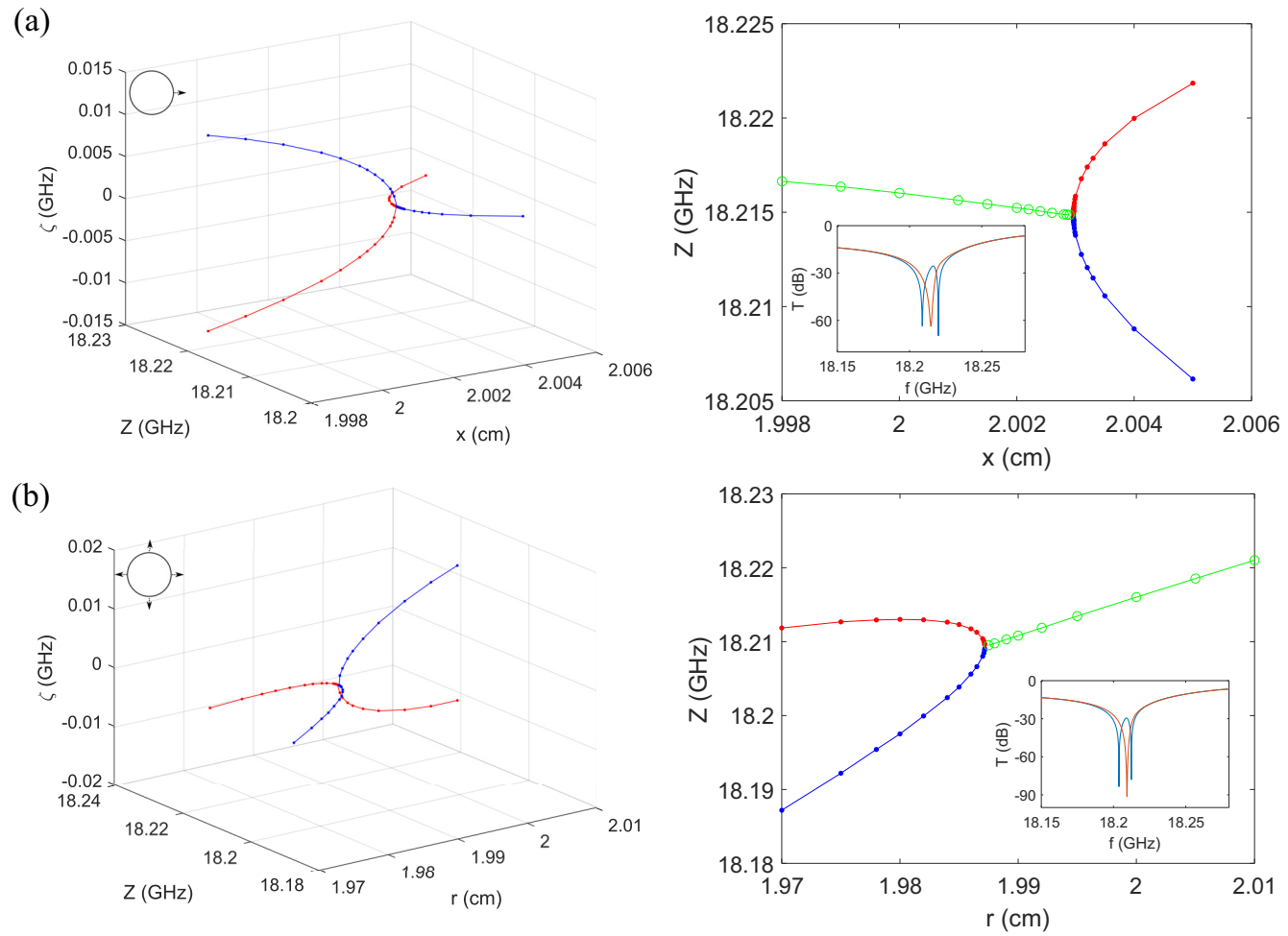

FIG. 3. Sensitivity of near degenerate transmission zeros in lossless billiard. (a) Left panel shows the trajectory of two T-zeros relative to the coordinate of the lowest disk. Right panel shows the variation of the frequency of the zeros with displacement of the disk. The green circles and the curve drawn through them give the real frequencies of the pair of T-zeros which meet at $x = 2.003$ cm. The trajectories for the two real zeros after they are created at $x \sim 2.003$ cm are shown in the red and blue curves. The red (blue) curve in the inset of the right panel shows the transmission spectrum when the x coordinate of the lowest disk is 2.003 (2.004) cm. (b) The trajectories of two transmission zeros with radius r of the lowest disk with center at $x = 2$ cm. Two curves meet at $r = 1.9872$ cm. The inset shows transmission spectra for a radius of the disk of 1.9872 cm (red) and 1.9850 cm (blue).

energy flow at the point that transmission vanished are shown in Fig. 2(a). This differs from the situation in a Fano resonance in which absorption disrupts zero transmission. The vanishing of transmission in an absorbing sample is easily perturbed since even a small perturbation moves the zero off the real axis. In contrast, a single zero in a Fano resonance in a lossless system cannot be moved off the real axis unless it meets a second single zero and the two are converted to a pair of zeros. This would be the time reversal of the scenario in Fig. 2(b). As was the case for the quasi-1D sample, transmission in the billiard can also be made to vanish by adding absorption (Sec. VI of the Supplemental Material [41]).

The first frame in Fig. 3(a) shows the evolution of two zeros in the complex plane as the lowest disk moves horizontally. The diverging slopes of the trajectories of the single and paired zeros relative to the x coordinate of the disk at the ZP indicates the diverging sensitivity of the T-zeros at the ZP. Near the ZP at $Z_0 = 18.2148$ GHz, $\zeta_0 = 0$ for $x_0 = 2.003$ cm, $|Z - Z_0| = \alpha_Z\sqrt{x - x_0}$, with $\alpha_Z = 0.17$ for the single zeros moving along the real axis, and $|\zeta - \zeta_0| = \alpha_\zeta\sqrt{x - x_0}$, with $\alpha_\zeta = 0.18$ for the conjugate pair moving perpendicular to the real axis. This gives the square root singularity in the sensitivities of Z and ζ around the ZP: $dZ/dx = \alpha_Z/2\sqrt{x - x_0}$ and $d\zeta/dx = \alpha_\zeta/2\sqrt{x - x_0}$. A comparison between transmission spectra in which the zeros are at (red) or near (blue) the ZP is shown in the inset in Fig. 3(a). A displacement of the lowest disk of 0.001 cm produces a 0.01 GHz shift between the transmission dips, which is a fractional shift of 5×10^{-4}. Figure 3(b) shows the sensitivity of the zeros relative to change of the radius of the lowest disk, for which the sensitivity of Z and ζ have a square root divergence at the ZP with $\alpha_Z = 0.11$ and $\alpha_\zeta = 0.09$. Thus, an easily resolved separation between the transmission dips is produced by a fractional change of $\sim$0.1% of the diameter of the disk. This translates to a layer of thickness 0.2 nm for a disk of 200 nm in a structure on an optical scale. Since the dips are clearly resolved, a thickness change which is a small fraction of an atomic diameter could be detected.

II. DISCUSSION

This paper explores the vanishing scattering coefficients. We have shown that the transmission and transmission time in complex structures are determined by the zeros as well as the poles of the TM. In addition to sharp dips in transmission when a T-zero is on the real axis, ultranarrow Lorentzian dips and peaks in transmission time can be created by positioning a T-zero slightly off the real axis. Unlike the zeros of the SM or RM, there are strong topological constraints on the positions and motion of zeros of the TM in the complex plane: In unitary media, T-zeros either lie on the real axis of the complex energy plane or are conjugate pairs. There is a square root singularity in the sensitivity of T-zeros to deformation at a ZP at which two single and a conjugate pair of T-zeros interconvert.

The present results show that transmission can vanish in both single and multichannel systems. Thus, the dynamic range of transmission eigenvalues is not limited in principle. The T-zeros give a general approach to vanishing transmission which is not limited by absorption, but in which absorption can be used to produce vanishing transmission.

This paper opens many questions such as the statistics of T-zeros, including the ratio of the number of single and paired zeros and the distribution of the imaginary coordinate of the paired zeros in structured and random systems. The distribution of zeros of the SM has been calculated in chaotic cavities [56]. The impact of nonuniformity in the imaginary part of the dielectric constant is still to be considered.

Extreme sensitivity is also found near EPs [2,35,57]. However, the high sensitivity of T-zeros near a ZP does not require the precise tuning of dissipation and/or gain for modes of the medium to coalesce as is required for EPs [2,35,57–59]. The ability to control the position of T-zeros by adding loss or gain or by deforming the sample, combined with the diverging sensitivity of T-zeros near a ZP, suggests that T-zeros may be exploited for ultrasensitive monitoring of structural change.

All data needed to evaluate the conclusions in the paper are presented in the paper and/or the Supplemental Material [41]. Additional data related to this paper will be supplied by the authors upon reasonable request.

ACKNOWLEDGMENTS

We thank Yiming Huang for sharing results of simulations and for valuable discussions. This paper is supported by the National Science Foundation under EAGER Award No. 2022629 and by PSC-CUNY under Award No. 63822-00 51.

The authors declare no competing interests.

[1] S. Longhi, PT-symmetric laser absorber, Phys. Rev. A **82**, 031801 (2010).

[2] M.-A. Miri and A. Alù, Exceptional points in optics and photonics, Science **363**, eaar7709 (2019).

[3] A. Krasnok, D. Baranov, H. Li, M.-A. Miri, F. Monticone, and A. Alú, Anomalies in light scattering, Adv. Opt. Photonics **11**, 892 (2019).

[4] W. R. Sweeney, C. W. Hsu, and A. D. Stone, Theory of reflectionless scattering modes, Phys. Rev. A **102**, 063511 (2020).

[5] Y. D. Chong, L. Ge, H. Cao, and A. D. Stone, Coherent Perfect Absorbers: Time-Reversed Lasers, Phys. Rev. Lett. **105**, 053901 (2010).

[6] W. Wan, Y. Chong, L. Ge, H. Noh, A. D. Stone, and H. Cao, Time-reversed lasing and interferometric control of absorption, Science **331**, 889 (2011).

[7] K. Pichler, M. Kühmayer, J. Böhm, A. Brandstötter, P. Ambichl, U. Kuhl, and S. Rotter, Random anti-lasing through coherent perfect absorption in a disordered medium, Nature **567**, 351 (2019).

[8] H. Li, S. Suwunnarat, R. Fleischmann, H. Schanz, and T. Kottos, Random Matrix Theory Approach to Chaotic Coherent Perfect Absorbers, Phys. Rev. Lett. **118**, 044101 (2017).

[9] P. del Hougne, K. B. Yeo, P. Besnier, and M. Davy, On-demand coherent perfect absorption in complex scattering systems: time delay divergence and enhanced sensitivity to perturbations, arXiv:2010.06438.

[10] L. Chen, T. Kottos, and S. M. Anlage, Perfect absorption in complex scattering systems with or without hidden symmetries, Nat. Commun. **11**, 5826 (2020).

[11] Y. D. Chong, L. Ge, and A. D. Stone, PT-Symmetry Breaking and Laser-Absorber Modes in Optical Scattering Systems, Phys. Rev. Lett. **106**, 093902 (2011).

[12] H. Li, A. Mekawy, A. Krasnok, and A. Alù, Virtual Parity-Time Symmetry, Phys. Rev. Lett. **124**, 193901 (2020).

[13] A.-S. B.-B. Dhia, L. Chesnel, and V. Pagneux, Trapped modes and reflectionless modes as eigenfunctions of the same spectral problem, Proc. R. Soc. A **474**, 20180050 (2018).

[14] Y. Fyodorov, Reflection time difference as a probe of S-matrix zeroes in chaotic resonance scattering, Acta Phys. Pol. A **136**, 785 (2019).

[15] M. Osman and Y. V. Fyodorov, Chaotic scattering with localized losses: S-matrix zeros and reflection time difference for systems with broken time-reversal invariance, Phys. Rev. E **102**, 012202 (2020).

[16] Y. V. Fyodorov and H.-J. Sommers, Statistics of resonance poles, phase shifts and time delays in quantum chaotic scattering: random matrix approach for systems with broken time-reversal invariance, J. Math. Phys. **38**, 1918 (1997).

[17] O. N. Dorokhov, On the coexistence of localized and extended electronic states in the metallic phase, Solid State Commun. **51**, 381 (1984).

[18] I. M. Vellekoop and A. P. Mosk, Focusing coherent light through opaque strongly scattering media, Opt. Lett. **32**, 2309 (2007).

[19] S. M. Popoff, G. Lerosey, R. Carminati, M. Fink, A. C. Boccara, and S. Gigan, Measuring the Transmission Matrix in Optics: An Approach to the Study and Control of Light Propagation in Disordered Media, Phys. Rev. Lett. **104**, 100601 (2010).

[20] H. Yu, T. R. Hillman, W. Choi, J. O. Lee, M. S. Feld, R. R. Dasari, and Y. Park, Measuring Large Optical Transmission Matrices of Disordered Media, Phys. Rev. Lett. **111**, 153902 (2013).

[21] S. M. Popoff, A. Goetschy, S. F. Liew, A. D. Stone, and H. Cao, Coherent Control of Total Transmission of Light

through Disordered Media, Phys. Rev. Lett. **112**, 133903 (2014).
[22] B. Gérardin, J. Laurent, A. Derode, C. Prada, and A. Aubry, Full Transmission and Reflection of Waves Propagating through a Maze of Disorder, Phys. Rev. Lett. **113**, 173901 (2014).
[23] S. Rotter and S. Gigan, Light fields in complex media: mesoscopic scattering meets wave control, Rev. Mod. Phys. **89**, 015005 (2017).
[24] U. Fano, Effects of configuration interaction on intensities and phase shifts, Phys. Rev. **124**, 1866 (1961).
[25] M. F. Limonov, M. V. Rybin, A. N. Poddubny, and Y. S. Kivshar, Fano resonances in photonics, Nat. Photonics **11**, 543 (2017).
[26] A. E. Miroshnichenko, S. Flach, and Y. S. Kivshar, Fano resonances in nanoscale structures, Rev. Mod. Phys. **82**, 2257 (2010).
[27] C. Wu, A. B. Khanikaev, R. Adato, N. Arju, A. A. Yanik, H. Altug, and G. Shvets, Fano-resonant asymmetric metamaterials for ultrasensitive spectroscopy and identification of molecular monolayers, Nat. Mater. **11**, 69 (2012).
[28] F. Zangeneh-Nejad and R. Fleury, Topological Fano Resonances, Phys. Rev. Lett. **122**, 014301 (2019).
[29] J. W. Yoon, M. J. Jung, S. H. Song, and R. Magnusson, Analytic theory of the resonance properties of metallic nanoslit arrays, IEEE J. Quantum Electron. **48**, 852 (2012).
[30] J.-L. Pichard, N. Zanon, Y. Imry, and A. D. Stone, Theory of random multiplicative transfer matrices and its implications for quantum transport, J. Phys. **51**, 587 (1990).
[31] C. W. J. Beenakker, Random-matrix theory of quantum transport, Rev. Mod. Phys. **69**, 731 (1997).
[32] Z. Shi and A. Z. Genack, Dynamic and spectral properties of transmission eigenchannels in random media, Phys. Rev. B **92**, 184202 (2015).
[33] P. A. Mello, P. Pereyra, and N. Kumar, Macroscopic approach to multichannel disordered conductors, Ann. Phys. **181**, 290 (1988).
[34] J. Wiersig, Enhancing the Sensitivity of Frequency and Energy Splitting Detection by Using Exceptional Points: Application to Microcavity Sensors for Single-Particle Detection, Phys. Rev. Lett. **112**, 203901 (2014).
[35] H. Hodaei, A. U. Hassan, S. Wittek, H. Garcia-Gracia, R. El-Ganainy, D. N. Christodoulides, and M. Khajavikhan, Enhanced sensitivity at higher-order exceptional points, Nature **548**, 187 (2017).
[36] E. P. Wigner, Lower limit for the energy derivative of the scattering phase shift, Phys. Rev. **98**, 145 (1955).
[37] F. T. Smith, Lifetime matrix in collision theory, Phys. Rev. **118**, 349 (1960).
[38] Y. Avishai and Y. B. Band, One-dimensional density of states and the phase of the transmission amplitude, Phys. Rev. B **32**, 2674 (1985).
[39] A. Z. Genack, P. Sebbah, M. Stoytchev, and B. A. van Tiggelen, Statistics of Wave Dynamics in Random Media, Phys. Rev. Lett. **82**, 715 (1999).
[40] C. Texier and A. Comtet, Universality of the Wigner Time Delay Distribution for One-Dimensional Random Potentials, Phys. Rev. Lett. **82**, 4220 (1999).
[41] See Supplemental Material at http://link.aps.org/supplemental/10.1103/PhysRevB.103.L100201 for (1) relation between transmission time and density of states, (2) expression for the determinant of the transmission matrix, (3) interference between two modes, (4) interference between a single mode and a continuum, (5) spectrum of the transmission time, and (6) transmissionless mode realized by adding absorption.
[42] M. Sh. Birman and M. G. Krein, On the theory of wave operators and scattering operators, Dokl. Akad. Nauk SSSR **144**, 475 (1962).
[43] M. Davy, Z. Shi, J. Wang, X. Cheng, and A. Z. Genack, Transmission Eigenchannels and the Densities of States of Random Media, Phys. Rev. Lett. **114**, 033901 (2015).
[44] F.-M. Dittes, The decay of quantum systems with a small number of open channels, Phys. Rep. **339**, 215 (2000).
[45] J. J. M. Verbaarschot, H. A. Weidenmüller, and M. R. Zirnbauer, Grassmann integration in stochastic quantum physics: the case of compound-nucleus scattering, Phys. Rep. **129**, 367 (1985).
[46] I. Rotter, Effective Hamiltonian and unitarity of the S matrix, Phys. Rev. E **68**, 016211 (2003).
[47] I. Rotter, A non-Hermitian Hamilton operator and the physics of open quantum systems, J. Phys. Math. Theor. **42**, 153001 (2009).
[48] D. S. Bernstein, *Scalar, Vector, and Matrix Mathematics* (Princeton University Press, Princeton, NJ, 2018).
[49] R. El-Ganainy, K. G. Makris, M. Khajavikhan, Z. H. Musslimani, S. Rotter, and D. N. Christodoulides, Non-Hermitian physics and PT symmetry, Nat. Phys. **14**, 11 (2018).
[50] C. W. Groth, M. Wimmer, A. R. Akhmerov, and X. Waintal, Kwant: A software package for quantum transport, New J. Phys. **16**, 063065 (2014).
[51] J. F. Nye and M. V. Berry, Dislocations in wave trains, Proc. R. Soc. A **336**, 165 (1974).
[52] M. V. Berry and M. R. Dennis, Phase singularities in isotropic random waves, Proc. R. Soc. A **456**, 2059 (2000).
[53] S. Zhang, B. Hu, P. Sebbah, and A. Z. Genack, Speckle Evolution of Diffusive and Localized Waves, Phys. Rev. Lett. **99**, 063902 (2007).
[54] V. A. Mandelshtam and H. S. Taylor, Spectral Analysis of Time Correlation Function for a Dissipative Dynamical System Using Filter Diagonalization: Application to Calculation of Unimolecular Decay Rates, Phys. Rev. Lett. **78**, 3274 (1997).
[55] J. Wiersig and J. Main, Fractal Weyl law for chaotic microcavities: Fresnel's laws imply multifractal scattering, Phys. Rev. E **77**, 036205 (2008).
[56] Y. V. Fyodorov, S. Suwunnarat, and T. Kottos, Distribution of zeros of the S-matrix of chaotic cavities with localized losses and coherent perfect absorption: non-perturbative results, J. Phys. Math. Theor. **50**, 30LT01 (2017).
[57] A. Guo, G. J. Salamo, D. Duchesne, R. Morandotti, M. Volatier-Ravat, V. Aimez, G. A. Siviloglou, and D. N. Christodoulides, Observation of PT-Symmetry Breaking in Complex Optical Potentials, Phys. Rev. Lett. **103**, 093902 (2009).
[58] C. M. Bender and S. Boettcher, Real Spectra in Non-Hermitian Hamiltonians Having PT Symmetry, Phys. Rev. Lett. **80**, 5243 (1998).
[59] C. E. Rüter, K. G. Makris, R. El-Ganainy, D. N. Christodoulides, M. Segev, and D. Kip, Observation of parity-time symmetry in optics, Nat. Phys. **6**, 192 (2010).